数理解析研究所講究録
1495 巻 2006 年 118-136

Cylindrical Couette flow of a vapor-gas mixture: A ghost effect in the continuum limit

Hiroaki Yoshida
Department of Aeronautics and Astronautics, Graduate School of Engineering, Kyoto University, Kyoto 606-8501, Japan

Kazuo Aoki
Department of Mechanical Engineering and Science, Graduate School of Engineering, Kyoto University, Kyoto 606-8501, Japan

Dedicated to Prof. Tai-Ping Liu on his 60th birthday

A binary mixture of gases is confined in a gap between two coaxial circular cylinders rotating at different angular velocities. One of the component gases is the vapor of the substance that forms the cylinders, so that evaporation or condensation (or sublimation) of the vapor may take place on the surfaces of the cylinders. The other component is a noncondensable gas that neither evaporates nor condenses on the surfaces. Axisymmetric and axially uniform flows (the cylindrical Couette flow) of such a mixture are investigated on the basis of kinetic theory with special interest in the continuum (or fluid-dynamic) limit in which the Knudsen number goes to zero. The fluid-dynamic system that describes the behavior of the mixture is derived by a formal but systematic asymptotic analysis of the Boltzmann system. The resulting system shows some nontrivial effects such as the ghost effect and the flow bifurcation.

1. INTRODUCTION

Axisymmetric and axially uniform flow between two rotating coaxial circular cylinders is a textbook example known as cylindrical Couette flow in classical fluid dynamics. It is also one of the basic flows for a rarefied gas and has been investigated on the basis of kinetic theory (see, for example, [1–4]). The flow is a simple time-independent and spatially one-dimensional flow, and it exhibits neither instability nor bifurcation unless the axial uniformity is released. However, if the gas is a vapor of the substance that forms the cylinders and it undergoes evaporation or condensation (or sublimation) on the surfaces of the cylinders, the situation changes dramatically. The flow exhibits bifurcation for relatively small Knudsen numbers even under the constraint of axial uniformity [5–8]. That is, there appear two or more different solutions for a certain range of parameters, such as the rotation speeds, the radii of the cylinders, and the Knudsen number. The structure of this bifurcation was investigated in detail by a formal but systematic asymptotic analysis of the Boltzmann equation with a delicate parameter setting in the case of slow rotation and small Knudsen numbers, and the essential features of the bifurcation were clarified [7]. One of the cases considered in Ref. [7] was then investigated mathematically in Ref. [9], and a rigorous proof of the existence of the bifurcation in the asymptotic limit was given.

Now let us consider the continuum (or fluid-dynamic) limit where the Knudsen number goes to zero in the case with evaporation and condensation on the cylinders. When the inner cylinder is rotating and the outer cylinder is at rest, there appear three different types of solution in a wide parameter range. First type exhibits evaporation on the inner cylinder and condensation on the outer, the second type condensation on the inner cylinder and evaporation on the outer, and the last type no evaporation or condensation on the cylinders [5]. The first and second types are described by the Euler equations with appropriate boundary conditions for evaporation and condensation [10]. For the third type, since there is no evaporation or condensation, it is natural to think that the flow field between the cylinders is the same as that of the ordinary cylindrical Couette flow. It is, however, not correct. The infinitesimal evaporation and condensation in this case have a significant effect on the flow field, such as the tangential velocity and temperature fields [12]. This is an example of the ghost effect that was discovered in Ref. [11] and investigated extensively in successive papers (see, e.g., Refs. [12–18]). The fluid-dynamic system that describes the third-type solution was derived systematically from the Boltzmann equation in Ref. [12], and the deformation of the tangential component of the flow velocity caused by the ghost effect was clarified. Direct numerical analysis of the Boltzmann equation or its model equation for very small Knudsen numbers was able to give numerical solutions that correspond to the first and the second

type mentioned above [5, 6, 8]. However, it could not show the solution corresponding to the third type [5, 6], most probably because of the instability of the solution. When the outer cylinder is rotating and the inner cylinder is at rest, there is no bifurcation of the flow in the continuum limit, and the solution without evaporation or condensation (i.e., the solution with the gost effect) appears for the rotation speed higher than a critical value. The solution corresponding to this solution was obtained by the direct numerical analysis for small Knudsen numbers [5, 12].

In the present study, we consider the same problem, the cylindrical Couette flow of the vapor with evaporation and condensation on the surfaces of the cylinders. The difference from the previous study is that we consider the case where another noncondensable gas, which neither evaporates nor condenses on the surfaces of the cylinders, is also contained in the gap of the two cylinders. According to the study of the plane Couette flow of the mixture of a vapor and a noncondensable gas [19], we can expect, in the cylindrical Couette flow, that evaporation and condensation are blocked by the noncondensable gas and vanish in the continuum limit in any parameter range. Therefore, the solution that exhibits the ghost effect caused by the infinitesimal evaporation and condensation is the natural and only possible solution when there is the noncondensable gas. We investigate this problem and derive the fluid-dynamic system that describes the behavior of the mixture in the continuum limit by a systematic asymptotic analysis of the Boltzmann system. As expected, the resulting fluid-dynamic system shows the ghost effect. More specifically, although evaporation and condensation of the vapor vanish in the continuum limit, it changes the flow field, such as the profile of the tangential component of the flow velocity, dramatically. In addition, such type of solution exhibits bifurcation in a certain parameter range. The ghost effect as well as the bifurcation of solution is investigated in detail on the basis of the numerical solution of the fluid-dynamic system. Furthermore, these results are compared with the Monte Carlo simulation of the Boltzmann equation for small Knudsen numbers.

2. FORMULATION OF THE PROBLEM

2.1. Problem

Let us consider a binary mixture of a vapor (A-component) and a noncondensable gas (B-component) confined in the gap between two coaxial circular cylinders made of the condensed phase of the vapor, rotating at different angular velocities. The vapor may evaporate or condense on the surfaces of the cylinders, whereas the noncondensable gas undergoes ordinary reflection without evaporation or condensation there. The radius, temperature, and surface velocity of the inner cylinder are denoted by L_I, T_I, and V_I, respectively, and the corresponding quantities of the outer cylinder by L_{II}, T_{II}, and V_{II}.

Restricting ourselves to the case of axisymmetric and axially uniform flows, we investigate the steady behavior of the mixture on the basis of the Boltzmann equation with special interest in the continuum limit where the Knudsen number vanishes.

2.2. Basic equations

Let us introduce the cylindrical coordinate system (r, θ, z) with the z axis along the common axis of the cylinders. Let $\boldsymbol{\xi}$ be the molecular velocity and ξ_r, ξ_θ, and ξ_z its r, θ, and z components, $F^\alpha(r, \boldsymbol{\xi})$ the velocity distribution function of the molecules of the α-component ($\alpha = A, B$). In what follows, we will use the indices α and β to represent the components of the mixture, i.e., $\alpha, \beta = A, B$.

The Boltzmann equation in the present problem is written in the following form:

$$\xi_r \frac{\partial F^\alpha}{\partial r} + \frac{\xi_\theta^2}{r}\frac{\partial F^\alpha}{\partial \xi_r} - \frac{\xi_r \xi_\theta}{r}\frac{\partial F^\alpha}{\partial \xi_\theta} = \sum_{\beta=A,B} J^{\beta\alpha}(F^\beta, F^\alpha), \tag{1}$$

where $J^{\beta\alpha}$ is the collision integral defined by:

$$J^{\beta\alpha}(F, G) = \int [F(\boldsymbol{\xi}_*')G(\boldsymbol{\xi}') - F(\boldsymbol{\xi}_*)G(\boldsymbol{\xi})]B^{\beta\alpha}(|\mathbf{e}\cdot\boldsymbol{V}|/V, V)\mathrm{d}\Omega(\mathbf{e})\mathrm{d}\boldsymbol{\xi}_*, \tag{2}$$

with

$$\boldsymbol{\xi}' = \boldsymbol{\xi} + \frac{\mu^{\beta\alpha}}{m^\alpha}(\mathbf{e}\cdot\boldsymbol{V})\mathbf{e}, \quad \boldsymbol{\xi}_*' = \boldsymbol{\xi}_* - \frac{\mu^{\beta\alpha}}{m^\beta}(\mathbf{e}\cdot\boldsymbol{V})\mathbf{e}, \tag{3}$$

$$\boldsymbol{V} = \boldsymbol{\xi}_* - \boldsymbol{\xi}, \quad V = |\boldsymbol{V}|, \quad \mu^{\beta\alpha} = \frac{2m^\alpha m^\beta}{m^\alpha + m^\beta}. \tag{4}$$

Here, $\boldsymbol{\xi}_*$ is the integration variable corresponding to $\boldsymbol{\xi}$, and $\mathrm{d}\boldsymbol{\xi}_* = \mathrm{d}\xi_{*r}\mathrm{d}\xi_{*\theta}\mathrm{d}\xi_{*z}$; $\mathbf{e}$ is the unit vector and $\mathrm{d}\Omega(\mathbf{e})$ is the solid-angle element in its direction; m^α is the mass of a molecule of the α-component; the domain of integration with respect to $\mathbf{e}$ is all direction, and that with respect to $\boldsymbol{\xi}_*$ is its whole space; $B^{\beta\alpha}(|\mathbf{e}\cdot\boldsymbol{V}|/V, V)$ is a nonnegative function of $|\mathbf{e}\cdot\boldsymbol{V}|/V$ and V, whose functional form is determined by the intermolecular force.

In order to describe the boundary condition on the cylinders, we need to introduce the saturation number densities n_I and n_{II} of the vapor molecules at temperatures T_I and T_{II}, respectively. For each substance, the saturation vapor pressure (or number density) is a function of the temperature only, determined by the Clausius–Clapeyron relation. Thus, n_I and n_{II} are determined by T_I and T_{II}, respectively. However, we can regard n_I and n_{II} as parameters independent of T_I and T_{II} if we keep the freedom of choosing substance of the vapor. For the purpose of describing the boundary conditions on the inner and outer cylinders in a unified fashion, we define the symbols σ_w, n_w, V_w, and T_w by

$$\begin{aligned} &\sigma_w = 1, \quad n_w = n_I, \quad V_w = V_I, \quad T_w = T_I, \qquad \text{at } r = L_I, \\ &\sigma_w = -1, \quad n_w = n_{II}, \quad V_w = V_{II}, \quad T_w = T_{II}, \qquad \text{at } r = L_{II}. \end{aligned} \tag{5}$$

The boundary conditions at $r = L_I$ and L_{II} are expressed in the following form [15, 20, 21]:

$$F^\alpha = g_w^\alpha(\boldsymbol{\xi}) + \int_{\sigma_w\xi_{*r}<0} K_w^\alpha(\boldsymbol{\xi}, \boldsymbol{\xi}_*)F^\alpha(r, \boldsymbol{\xi}_*)\mathrm{d}\boldsymbol{\xi}_*, \quad (\text{for } \sigma_w\xi_r > 0), \tag{6}$$

where the source term $g_w^\alpha(\boldsymbol{\xi})$ and the scattering kernel $K_w^\alpha(\boldsymbol{\xi}, \boldsymbol{\xi}_*)$ are given functions, the functional forms of which are determined by the nature of the boundary. The $g_w^\alpha(\boldsymbol{\xi})$ and $K_w^\alpha(\boldsymbol{\xi}, \boldsymbol{\xi}_*)$ need to satisfy the following conditions:

$$g_w^A(\boldsymbol{\xi}) \geq 0, \qquad (\sigma_w\xi_r > 0), \tag{7a}$$

$$g_w^B(\boldsymbol{\xi}) = 0, \qquad (\sigma_w\xi_r > 0), \tag{7b}$$

$$K_w^\alpha(\boldsymbol{\xi}, \boldsymbol{\xi}_*) \geq 0, \qquad (\sigma_w\xi_r > 0, \quad \sigma_w\xi_{*r} < 0), \tag{7c}$$

$$\int_{\sigma_w\xi_r>0} |\xi_r/\xi_{*r}|K_w^B(\boldsymbol{\xi}, \boldsymbol{\xi}_*)\mathrm{d}\boldsymbol{\xi} = 1, \qquad (\sigma_w\xi_{*r} < 0), \tag{7d}$$

where Eq. (7d) indicates that there is no net particle flux of the B-component across the surface of the cylinders, that is, the B-component is noncondensable. In the present problem, g_w^A and K_w^A depend on n_w, V_w, T_w, and m^A, and K_w^B on V_w, T_w, and m^B. We assume that Eq. (6) is satisfied by the wall-state equilibrium distributions, i.e.,

$$F_w^\alpha = g_w^\alpha(\boldsymbol{\xi}) + \int_{\sigma_w\xi_{*r}<0} K_w^\alpha(\boldsymbol{\xi}, \boldsymbol{\xi}_*)F_w^\alpha(\boldsymbol{\xi}_*)\mathrm{d}\boldsymbol{\xi}_*, \tag{8}$$

with

$$F_w^A = \frac{n_w}{(2\pi k_B T_w/m^A)^{3/2}} \exp\left(-\frac{\xi_r^2 + (\xi_\theta - V_w)^2 + \xi_z^2}{2k_B T_w/m^A}\right), \tag{9a}$$

$$F_w^B = \frac{c}{(2\pi k_B T_w/m^B)^{3/2}} \exp\left(-\frac{\xi_r^2 + (\xi_\theta - V_w)^2 + \xi_z^2}{2k_B T_w/m^B}\right), \tag{9b}$$

where c is an arbitrary constant, and k_B is the Boltzmann constant. We also assume that Eqs. (9a) and (9b) are the only equilibrium distributions that satisfy Eq. (8).

Let n^α, $v^\alpha = (v_r^\alpha, v_\theta^\alpha, 0)$, p^α, and T^α be the molecular number density, the flow velocity, the pressure, and the temperature of the α-component. These macroscopic quantities are expressed in terms of the velocity distribution functions as

$$n^\alpha = \int F^\alpha \mathrm{d}\boldsymbol{\xi}, \tag{10a}$$

$$v_r^\alpha = \frac{1}{n^\alpha}\int \xi_r F^\alpha \mathrm{d}\boldsymbol{\xi}, \qquad v_\theta^\alpha = \frac{1}{n^\alpha}\int \xi_\theta F^\alpha \mathrm{d}\boldsymbol{\xi}, \tag{10b}$$

$$p^\alpha = k_B n^\alpha T^\alpha = \frac{1}{3}\int m^\alpha[(\xi_r - v_r^\alpha)^2 + (\xi_\theta - v_\theta^\alpha)^2 + \xi_z^2]F^\alpha \mathrm{d}\boldsymbol{\xi}, \tag{10c}$$

where $\mathrm{d}\boldsymbol{\xi} = \mathrm{d}\xi_r \mathrm{d}\xi_\theta \mathrm{d}\xi_z$. In Eqs. (10a)-(10c) and in what follows, the domain of integration with respect to $\boldsymbol{\xi}$ is its whole space unless the contrary is stated. The number density n, the mass density ρ, the flow velocity $\boldsymbol{v} = (v_r, v_\theta, 0)$, the pressure p, and the temperature T of the total mixture are defined by

$$n = \int (F^A + F^B)\mathrm{d}\boldsymbol{\xi}, \tag{11a}$$

$$\rho = \int (m^A F^A + m^B F^B)\mathrm{d}\boldsymbol{\xi}, \tag{11b}$$

$$v_r = \frac{1}{\rho}\int \xi_r (m^A F^A + m^B F^B)\mathrm{d}\boldsymbol{\xi}, \tag{11c}$$

$$v_\theta = \frac{1}{\rho}\int \xi_\theta (m^A F^A + m^B F^B)\mathrm{d}\boldsymbol{\xi}, \tag{11d}$$

$$p = k_B n T = \frac{1}{3}\int [(\xi_r - v_r)^2 + (\xi_\theta - v_\theta)^2 + \xi_z^2](m^A F^A + m^B F^B)\mathrm{d}\boldsymbol{\xi}. \tag{11e}$$

Therefore, they are expressed in terms of the macroscopic quantities of each component as

$$n = n^A + n^B, \tag{12a}$$

$$\rho = m^A n^A + m^B n^B, \tag{12b}$$

$$v_r = (m^A n^A v_r^A + m^B n^B v_r^B)/\rho, \tag{12c}$$

$$v_\theta = (m^A n^A v_\theta^A + m^B n^B v_\theta^B)/\rho, \tag{12d}$$

$$p = \sum_{\alpha=A,B} [p^\alpha + m^\alpha n^\alpha (v_r^\alpha - v_r)^2/3 + m^\alpha n^\alpha (v_\theta^\alpha - v_\theta)^2/3]. \tag{12e}$$

To complete the physical setting of the problem, we need to specify a quantity associated with the amount of the noncondensable gas. As this parameter, we choose the average number density of the noncondensable gas,

$$n_{av}^B = \frac{1}{\pi(L_{II}^2 - L_I^2)}\int_{-\pi}^{\pi}\int_{L_I}^{L_{II}}\int r F^B \mathrm{d}\boldsymbol{\xi}\mathrm{d}r\mathrm{d}\theta. \tag{13}$$

By integrating both sides of Eq. (1) with respect to $\boldsymbol{\xi}$ over its whole space, we obtain

$$r n^\alpha v_r^\alpha = \text{const}, \tag{14}$$

which expresses the mass conservation for each component gas. On the other hand, if we integrate Eq. (6) (with $\alpha = B$) multiplied by ξ_r with respect to $\boldsymbol{\xi}$ over the space $\sigma_w \xi_r > 0$ and take Eq. (7d) into consideration, we obtain $n^B v_r^B = 0$ at $r = L_I$ and L_{II}. Thus we have

$$n^B v_r^B = 0, \qquad (L_I \le r \le L_{II}). \tag{15}$$

2.3. Dimensionless expressions

To derive the dimensionless expressions of the basic system, we introduce the following dimensionless variables:

$$\begin{aligned}
&\hat{r} = \frac{r}{L_I}, \quad \boldsymbol{\zeta} = (\zeta_r, \zeta_\theta, \zeta_z) = \frac{\boldsymbol{\xi}}{V_{th}}, \quad f^\alpha = \frac{V_{th}^3}{n_I} F^\alpha, \quad \hat{m}^\alpha = \frac{m^\alpha}{m^A}, \\
&\hat{n}^\alpha = \frac{n^\alpha}{n_I}, \quad \hat{\boldsymbol{v}}^\alpha = (\hat{v}_r^\alpha, \hat{v}_\theta^\alpha, 0) = \frac{\boldsymbol{v}^\alpha}{V_{th}}, \quad \hat{p}^\alpha = \frac{p^\alpha}{p_I}, \quad \hat{T}^\alpha = \frac{T^\alpha}{T_I}, \\
&\hat{n} = \frac{n}{n_I}, \quad \hat{\rho} = \frac{\rho}{\rho_I}, \quad \hat{\boldsymbol{v}} = (\hat{v}_r, \hat{v}_\theta, 0) = \frac{\boldsymbol{v}}{V_{th}}, \quad \hat{p} = \frac{p}{p_I}, \quad \hat{T} = \frac{T}{T_I},
\end{aligned} \tag{16}$$

where $V_{th} = (2k_B T_I/m^A)^{1/2}$ is the most probable speed of the molecules of the A-component in the equilibrium state at rest at temperature T_I; $\rho_I = m^A n_I$ and $p_I = k_B n_I T_I$ are, respectively, the density and the pressure of the vapor in the saturated equilibrium state at rest at temperature T_I.

Then the Boltzmann equation (1) becomes

$$\mathcal{D} f^\alpha = \frac{2}{\sqrt{\pi}\mathrm{Kn}} \sum_{\beta=A,B} K^{\beta\alpha} \hat{J}^{\beta\alpha}(f^\beta, f^\alpha), \tag{17}$$

$$\mathcal{D} = \zeta_r \frac{\partial}{\partial \hat{r}} + \frac{\zeta_\theta^2}{\hat{r}} \frac{\partial}{\partial \zeta_r} - \frac{\zeta_r \zeta_\theta}{\hat{r}} \frac{\partial}{\partial \zeta_\theta}, \tag{18}$$

$$\hat{J}^{\beta\alpha}(f, g) = \int [f(\boldsymbol{\zeta}_*') g(\boldsymbol{\zeta}') - f(\boldsymbol{\zeta}_*) g(\boldsymbol{\zeta})] \hat{B}^{\beta\alpha}(|\mathbf{e} \cdot \hat{\boldsymbol{V}}|/\hat{V}, \hat{V}) \mathrm{d}\Omega(\mathbf{e}) \mathrm{d}\boldsymbol{\zeta}_*, \tag{19}$$

$$\boldsymbol{\zeta}' = \boldsymbol{\zeta} + \frac{\hat{\mu}^{\beta\alpha}}{\hat{m}^\alpha} (\mathbf{e} \cdot \hat{\boldsymbol{V}}) \mathbf{e}, \quad \boldsymbol{\zeta}_*' = \boldsymbol{\zeta}_* - \frac{\hat{\mu}^{\beta\alpha}}{\hat{m}^\beta} (\mathbf{e} \cdot \hat{\boldsymbol{V}}) \mathbf{e}, \tag{20}$$

$$\hat{\boldsymbol{V}} = \boldsymbol{\zeta}_* - \boldsymbol{\zeta}, \quad \hat{V} = |\hat{\boldsymbol{V}}|, \quad \hat{\mu}^{\beta\alpha} = \frac{2\hat{m}^\alpha \hat{m}^\beta}{\hat{m}^\alpha + \hat{m}^\beta}, \tag{21}$$

$$\hat{B}^{\beta\alpha}(|\mathbf{e} \cdot \hat{\boldsymbol{V}}|/\hat{V}, \hat{V}) = \frac{B^{\beta\alpha}}{B_0^{\beta\alpha}}, \quad K^{\beta\alpha} = \frac{B_0^{\beta\alpha}}{B_0^{AA}}, \tag{22}$$

$$B_0^{\beta\alpha} = \frac{1}{n_I^2} \int F_0^\alpha(\boldsymbol{\xi}) F_0^\beta(\boldsymbol{\xi}_*) B^{\beta\alpha}(|\mathbf{e} \cdot \boldsymbol{V}|/V, V) \mathrm{d}\Omega(\mathbf{e}) \mathrm{d}\boldsymbol{\xi} \mathrm{d}\boldsymbol{\xi}_*, \tag{23}$$

$$F_0^\alpha = \frac{n_I}{(2\pi k_B T_I/m^\alpha)^{3/2}} \exp\left(-\frac{\xi_r^2 + \xi_\theta^2 + \xi_z^2}{2k_B T_I/m^\alpha}\right). \tag{24}$$

Here, $\boldsymbol{\zeta}_*$ is the integration variable corresponding to $\boldsymbol{\zeta}$, and $\mathrm{d}\boldsymbol{\zeta}_* = \mathrm{d}\zeta_{*r}\mathrm{d}\zeta_{*\theta}\mathrm{d}\zeta_{*z}$; the domain of integration is the whole space of $\boldsymbol{\zeta}_*$ and all directions of $\mathbf{e}$ [$\mathbf{e}$ and $\mathrm{d}\Omega(\mathbf{e})$ are the same as in Eq. (2)]; Kn on the right-hand side of Eq. (17) is the reference Knudsen number defined by $\mathrm{Kn} = \ell_0/L_I$, where $\ell_0 = 2V_{th}/\sqrt{\pi} n_I B_0^{AA}$ is the mean free path of the molecules of the vapor in the equilibrium state at rest with temperature T_I and molecular number density n_I.

When the intermolecular potential extends to infinity, the so-called angular cutoff is introduced in Eq. (23), that is, $B^{\beta\alpha}$ is set to be zero for the domain $|\mathbf{e} \cdot \boldsymbol{V}|/V \le \delta$ (δ: a specified constant), which corresponds to grazing collisions. It should be noted that the function $\hat{B}^{\beta\alpha}$ in general depends on the dimensionless parameter $U_0^{\beta\alpha}/k_B T_I$, where $U_0^{\beta\alpha}$ is the characteristic size of the intermolecular potential for the interaction of a molecule of the α-component with a molecule of the β-component [15]. This parameter is not shown explicitly in the above equations. When both component gases consist of hard-sphere molecules, $\hat{B}^{\beta\alpha}$ does not depend on this parameter, and $\hat{B}^{\beta\alpha}$, $K^{\beta\alpha}$, and ℓ_0 are given by

$$\hat{B}^{\beta\alpha} = \frac{(\hat{\mu}^{\beta\alpha})^{1/2}}{4\sqrt{2\pi}} |\mathbf{e} \cdot \hat{\boldsymbol{V}}|, \quad K^{\beta\alpha} = \frac{1}{(\hat{\mu}^{\beta\alpha})^{1/2}} \left(\frac{d^\beta + d^\alpha}{2d^A}\right)^2, \quad \ell_0 = \frac{1}{\sqrt{2}\pi (d^A)^2 n_I}, \tag{25}$$

where d^α is the diameter of a molecule of the α-component.

Corresponding to Eq. (5), we introduce the following symbols:

$$\begin{aligned} &\sigma_w = 1, \quad \hat{n}_w = 1, \quad \hat{V}_w = \frac{V_I}{V_{th}}, \quad \hat{T}_w = 1, \qquad \text{at } \hat{r} = 1, \\ &\sigma_w = -1, \quad \hat{n}_w = \frac{n_{II}}{n_I}, \quad \hat{V}_w = \frac{V_{II}}{V_{th}}, \quad \hat{T}_w = \frac{T_{II}}{T_I}, \qquad \text{at } \hat{r} = \frac{L_{II}}{L_I}. \end{aligned} \tag{26}$$

The dimensionless form of the boundary conditions is as follows: at $\hat{r} = 1$ and L_{II}/L_I,

$$f^\alpha = \hat{g}_w^\alpha(\boldsymbol{\zeta}) + \int_{\sigma_w \zeta_{*r} < 0} \hat{K}_w^\alpha(\boldsymbol{\zeta}, \boldsymbol{\zeta}_*) f^\alpha(\hat{r}, \boldsymbol{\zeta}_*) \mathrm{d}\boldsymbol{\zeta}_*, \qquad (\text{for } \sigma_w \zeta_r > 0), \tag{27}$$

where

$$\hat{g}_w^\alpha = \frac{V_{th}^3}{n_I} g_w^\alpha, \qquad \hat{K}_w^\alpha = V_{th}^3 K_w^\alpha, \tag{28}$$

and $\hat{g}_w^\alpha(\boldsymbol{\zeta})$ and $\hat{K}_w^\alpha(\boldsymbol{\zeta}, \boldsymbol{\zeta}_*)$ satisfy

$$\hat{g}_w^A(\boldsymbol{\zeta}) \geq 0, \qquad (\sigma_w \zeta_r > 0), \tag{29a}$$

$$\hat{g}_w^B(\boldsymbol{\zeta}) = 0, \qquad (\sigma_w \zeta_r > 0), \tag{29b}$$

$$\hat{K}_w^\alpha(\boldsymbol{\zeta}, \boldsymbol{\zeta}_*) \geq 0, \qquad (\sigma_w \zeta_r > 0,\ \sigma_w \zeta_{*r} < 0), \tag{29c}$$

$$\int_{\sigma_w \zeta_r > 0} |\zeta_r / \zeta_{*r}| \hat{K}_w^B(\boldsymbol{\zeta}, \boldsymbol{\zeta}_*) \mathrm{d}\boldsymbol{\zeta} = 1, \qquad (\sigma_w \zeta_{*r} < 0). \tag{29d}$$

In addition, corresponding to Eqs. (8)–(9b), we have

$$f_w^\alpha = \hat{g}_w^\alpha(\boldsymbol{\zeta}) + \int_{\sigma_w \zeta_{*r} < 0} \hat{K}_w^\alpha(\boldsymbol{\zeta}, \boldsymbol{\zeta}_*) f_w^\alpha(\boldsymbol{\zeta}_*) \mathrm{d}\boldsymbol{\zeta}_*, \tag{30}$$

$$f_w^A = \frac{\hat{n}_w}{(\pi \hat{T}_w)^{3/2}} \exp\left(-\frac{\zeta_r^2 + (\zeta_\theta - \hat{V}_w)^2 + \zeta_z^2}{\hat{T}_w} \right), \tag{31a}$$

$$f_w^B = \frac{\hat{c}}{(\pi \hat{T}_w / \hat{m}^B)^{3/2}} \exp\left(-\frac{\zeta_r^2 + (\zeta_\theta - \hat{V}_w)^2 + \zeta_z^2}{\hat{T}_w / \hat{m}^B} \right), \tag{31b}$$

where $\hat{c}$ is an arbitrary (dimensionless) constant.

It is seen from Eqs. (26) and (30)–(31b) that the parameters n_{II}/n_I, V_I/V_{th}, V_{II}/V_{th}, T_{II}/T_I, and m^B/m^A are contained in the boundary condition. In general, however, $\hat{g}_w^A$ and $\hat{K}_w^A$ also depend on the reference temperature T_I, the reference number density n_I, and the reference molecular mass m^A, and $\hat{K}_w^B$ also depends on T_I and m^A. In the case of the so-called complete condensation condition [15] for the vapor, and the diffuse reflection condition [15] for the noncondensable gas, $\hat{g}_w^\alpha$ and $\hat{K}_w^\alpha$ are given by

$$\hat{g}_w^A(\boldsymbol{\zeta}) = \frac{\hat{n}_w}{(\pi \hat{T}_w)^{3/2}} \exp\left(-\frac{\zeta_r^2 + (\zeta_\theta - \hat{V}_w)^2 + \zeta_z^2}{\hat{T}_w} \right), \tag{32}$$

$$\hat{g}_w^B(\boldsymbol{\zeta}) = 0, \tag{33}$$

$$\hat{K}_w^A(\boldsymbol{\zeta}, \boldsymbol{\zeta}_*) = 0, \tag{34}$$

$$\hat{K}_w^B(\boldsymbol{\zeta}, \boldsymbol{\zeta}_*) = -\frac{2}{\pi} \left(\frac{\hat{m}^B}{\hat{T}_w} \right)^2 \sigma_w \zeta_{*r} \exp\left(-\frac{\zeta_r^2 + (\zeta_\theta - \hat{V}_w)^2 + \zeta_z^2}{\hat{T}_w / \hat{m}^B} \right). \tag{35}$$

In this case, $\hat{g}_w^\alpha$ and $\hat{K}_w^\alpha$ depend only on n_{II}/n_I, V_I/V_{th}, V_{II}/V_{th}, T_{II}/T_I, and m^B/m^A and do not depend on T_I, n_I, or m^A.

The dimensionless version of the relations between the macroscopic variables and the velocity distribution functions, Eqs. (10)–(12) are given by

$$\hat{n}^\alpha = \int f^\alpha \mathrm{d}\boldsymbol{\zeta}, \tag{36a}$$

$$\hat{v}_r^\alpha = \frac{1}{\hat{n}^\alpha}\int \zeta_r f^\alpha \mathrm{d}\boldsymbol{\zeta}, \quad \hat{v}_\theta^\alpha = \frac{1}{\hat{n}^\alpha}\int \zeta_\theta f^\alpha \mathrm{d}\boldsymbol{\zeta}, \tag{36b}$$

$$\hat{p}^\alpha = \hat{n}^\alpha \hat{T}^\alpha = \frac{2}{3}\int \hat{m}^\alpha[(\zeta_r - \hat{v}_r^\alpha)^2 + (\zeta_\theta - \hat{v}_\theta^\alpha)^2 + \zeta_z^2] f^\alpha \mathrm{d}\boldsymbol{\zeta}, \tag{36c}$$

$$\hat{n} = \int (f^A + f^B)\mathrm{d}\boldsymbol{\zeta} = \hat{n}^A + \hat{n}^B, \tag{36d}$$

$$\hat{\rho} = \int \left(\hat{m}^A f^A + \hat{m}^B f^B\right) \mathrm{d}\boldsymbol{\zeta} = \hat{m}^A \hat{n}^A + \hat{m}^B \hat{n}^B, \tag{36e}$$

$$\hat{v}_r = \frac{1}{\hat{\rho}}\int \zeta_r \left(\hat{m}^A f^A + \hat{m}^B f^B\right) \mathrm{d}\boldsymbol{\zeta} = \frac{1}{\hat{\rho}}\left(\hat{m}^A \hat{n}^A \hat{v}_r^A + \hat{m}^B \hat{n}^B \hat{v}_r^B\right), \tag{36f}$$

$$\hat{v}_\theta = \frac{1}{\hat{\rho}}\int \zeta_\theta \left(\hat{m}^A f^A + \hat{m}^B f^B\right) \mathrm{d}\boldsymbol{\zeta} = \frac{1}{\hat{\rho}}\left(\hat{m}^A \hat{n}^A \hat{v}_\theta^A + \hat{m}^B \hat{n}^B \hat{v}_\theta^B\right), \tag{36g}$$

$$\begin{aligned}\hat{p} = \hat{n}\hat{T} &= \frac{2}{3}\int [(\zeta_r - \hat{v}_r)^2 + (\zeta_\theta - \hat{v}_\theta)^2 + \zeta_z^2] \left(\hat{m}^A f^A + \hat{m}^B f^B\right) \mathrm{d}\boldsymbol{\zeta} \\ &= \sum_{\alpha=A,B}\left[\hat{p}^\alpha + \frac{2}{3}\hat{m}^\alpha \hat{n}^\alpha (\hat{v}_r^\alpha - \hat{v}_r)^2 + \frac{2}{3}\hat{m}^\alpha n^\alpha (\hat{v}_\theta^\alpha - \hat{v}_\theta)^2\right],\end{aligned} \tag{36h}$$

where $\mathrm{d}\boldsymbol{\zeta} = \mathrm{d}\zeta_r \mathrm{d}\zeta_\theta \mathrm{d}\zeta_z$. Here and in what follows, the domain of integration with respect to $\boldsymbol{\zeta}$ is its whole space unless the contrary is stated.

The dimensionless forms of Eqs. (13)–(15) are, respectively,

$$\frac{n_{av}^B}{n_I} = \frac{2}{(L_{II}/L_I)^2 - 1}\int_1^{L_{II}/L_I} \hat{r}\hat{n}^B \mathrm{d}\hat{r}, \tag{37}$$

$$\hat{r}\hat{n}^A \hat{v}_r^A = \text{const} \quad \text{and} \quad \hat{n}^B \hat{v}_r^B = 0, \quad \text{for } 1 \le \hat{r} \le L_{II}/L_I. \tag{38}$$

3. ASYMPTOTIC ANALYSIS FOR SMALL KNUDSEN NUMBERS

In this section, we consider the case where the Knudsen number Kn is small and carry out a systematic asymptotic analysis of the boundary-value problem, Eqs. (17) and (27), following the asymptotic theory developed by Sone (see, e.g., Refs. [11, 12, 15, 22–24]) as a guideline. The analysis here can be carried out in a way parallel to Ref. [19]. For convenience, we use the following small parameter ϵ rather than Kn in this section:

$$\epsilon = (\sqrt{\pi}/2)\mathrm{Kn} \ll 1. \tag{39}$$

3.1. Fluid-dynamic equations and boundary conditions

First, we leave aside the boundary condition (27) and look for a moderately varying solution f_H^α, which satisfies $\partial f_H^\alpha/\partial \hat{r} = O(f_H^\alpha)$, in the form of a power series of ϵ:

$$f_H^\alpha = f_{H0}^\alpha + f_{H1}^\alpha \epsilon + \cdots. \tag{40}$$

This f_H^α is called the Hilbert solution or expansion. Substitution of Eq. (40) into Eqs. (36a)-(36h) gives the corresponding power series expansions of the macroscopic variables of each component and of the total mixture:

$$h_H^\alpha = h_{H0}^\alpha + h_{H1}^\alpha \epsilon + \cdots, \tag{41}$$

$$h_H = h_{H0} + h_{H1}\epsilon + \cdots, \tag{42}$$

where the letter h stands for $\hat{n}$, $\hat{v}$, $\hat{T}$, etc., and the subscript H indicates the quantities corresponding to the Hilbert solution. The coefficient functions h^{α}_{Hm} and h_{Hm} are expressed in terms of f^{α}_{Hn} $(n \leq m)$. Their explicit forms for $m = 0$ and 1 are given in Appendix A. After substituting Eq. (40) into Eq. (17) and arranging the power of ϵ, we obtain a series of integral equations for the coefficients f^{α}_{Hm}:

$$\sum_{\beta=A,B} K^{\beta\alpha}\hat{J}^{\beta\alpha}(f^{\beta}_{H0}, f^{\alpha}_{H0}) = 0, \tag{43}$$

$$\sum_{\beta=A,B} K^{\beta\alpha}[\hat{J}^{\beta\alpha}(f^{\beta}_{H0}, f^{\alpha}_{Hm}) + \hat{J}^{\beta\alpha}(f^{\beta}_{Hm}, f^{\alpha}_{H0})]$$

$$= \mathcal{D}f^{\alpha}_{Hm-1} - \sum_{l=1}^{m-1}\sum_{\beta=A,B} K^{\beta\alpha}\hat{J}^{\beta\alpha}(f^{\beta}_{Hl}, f^{\alpha}_{Hm-l}), \qquad (m = 1, 2, \ldots), \tag{44}$$

where $\sum_{l=1}^{m-1}$ is set to be zero when $m = 1$.

As is well known [25], the solution of Eq. (43) is a local Maxwellian distribution for each component with a common temperature and a common flow velocity. The solution is expressed in the following form using the leading order terms $\hat{n}^{\alpha}_{H0}$, $\hat{v}_{rH0}$, $\hat{v}_{\theta H0}$, and $\hat{T}_{H0}$ of the Hilbert expansion of the macroscopic quantities:

$$f^{\alpha}_{H0} = \frac{\hat{n}^{\alpha}_{H0}}{(\pi\hat{T}_{H0}/\hat{m}^{\alpha})^{3/2}} \exp\left(-\frac{(\zeta_r - \hat{v}_{rH0})^2 + (\zeta_\theta - \hat{v}_{\theta H0})^2 + \zeta_z^2}{\hat{T}_{H0}/\hat{m}^{\alpha}}\right). \tag{45}$$

This gives the obvious relations

$$\hat{v}^{A}_{rH0} = \hat{v}^{B}_{rH0} = \hat{v}_{rH0}, \qquad \hat{v}^{A}_{\theta H0} = \hat{v}^{B}_{\theta H0} = \hat{v}_{\theta H0}, \qquad \hat{T}^{A}_{H0} = \hat{T}^{B}_{H0} = \hat{T}_{H0}. \tag{46}$$

On the other hand, from Eq. (38) we have

$$\hat{n}^{B}_{H0}\hat{v}^{B}_{rH0} = 0, \qquad (1 \leq \hat{r} \leq L_{II}/L_I). \tag{47}$$

The case where $\hat{n}^{B}_{H0} \equiv 0$, i.e., there is no noncondensable gas in the leading order (of the Hilbert solution), has been investigated for general geometry in Ref. [26]. In this case, a small amount of the noncondensable gas is blown away by the vapor flow and pushed against the surface where condensation of the vapor is taking place. As a result, the noncondensable component of a very small amount accumulates in a very thin layer adjacent to the condensing surface and may have a significant effect on the global vapor flow [26–28]. In the present study, we consider the opposite case, i.e., the case where $\hat{n}^{B}_{H0} > 0$ in $1 \leq \hat{r} \leq L_{II}/L_I$ (the case where $\hat{n}^{B}_{H0}$ vanishes in a certain interval of $\hat{r}$ can be handled in the framework of the present analysis). Then, $\hat{v}^{B}_{rH0}$ vanishes identically, so that Eq. (46) gives

$$\hat{v}^{A}_{rH0} = \hat{v}^{B}_{rH0} = \hat{v}_{rH0} \equiv 0. \tag{48}$$

Therefore, the leading-order solution f^{α}_{II0} reduces to

$$f^{\alpha}_{H0} = \frac{\hat{n}^{\alpha}_{H0}}{(\pi\hat{T}_{H0}/\hat{m}^{\alpha})^{3/2}} \exp\left(-\frac{\zeta_r^2 + (\zeta_\theta - \hat{v}_{\theta H0})^2 + \zeta_z^2}{\hat{T}_{H0}/\hat{m}^{\alpha}}\right). \tag{49}$$

The mth-order equation, Eq. (44), is an inhomogeneous linear integral equation for f^{α}_{Hm}. Because of the form of Eq. (49), the left-hand side of Eq. (44) is essentially the linearized collision term for a binary mixture of gases. Therefore, the corresponding homogeneous equation has the independent nontrivial solutions: $(a^{\alpha}, \hat{m}^{\alpha}\boldsymbol{\zeta}, \hat{m}^{\alpha}\zeta^2)\, f^{\alpha}_{H0}$, where a^{α} are arbitrary constants, and $\zeta^2 = \zeta_r^2 + \zeta_\theta^2 + \zeta_z^2$. In consequence, in order that Eq. (44) has a solution, its inhomogeneous term should satisfy a certain solvability condition, which is reduced to the following form:

$$\int \mathcal{D}f^{\alpha}_{Hm-1}\mathrm{d}\boldsymbol{\zeta} = 0, \tag{50}$$

$$\int \sum_{\alpha=A,B} \hat{m}^{\alpha}\boldsymbol{\zeta}\mathcal{D}f^{\alpha}_{Hm-1}\mathrm{d}\boldsymbol{\zeta} = 0, \tag{51}$$

$$\int \sum_{\alpha=A,B} \hat{m}^{\alpha}\zeta^2\mathcal{D}f^{\alpha}_{Hm-1}\mathrm{d}\boldsymbol{\zeta} = 0. \tag{52}$$

If we insert Eq. (49) in Eqs. (50)–(52) with $m = 1$, the $\hat{r}$-component of Eq. (51) gives a constraint shown in Eq. (54) below, but other conditions are satisfied automatically. With this constraint, Eq. (44) with $m = 1$ can be solved. The explicit form of the solution f^{α}_{H1} is given in Appendix B. If we substitute this f^{α}_{H1} into Eqs. (50)–(52) with $m = 2$, we obtain some constraints for the macroscopic variables contained in f^{α}_{H1}. With these constraints, we can proceed to the higher order. In this way, the functional form of f^{α}_{Hn} with respect to ζ is determined successively ($n = 0, 1, \ldots$), and at the same time the constraints on the (unknown) macroscopic variables h^{α}_{Hn} and h_{Hn} are obtained in the form of ordinary differential equations. The latter equations are the so-called fluid-dynamic equations. The set of equations necessary to determine the leading-order solution f^{α}_{H0} is essentially obtained from Eq. (50) with $m = 2$, the $\hat{r}$-component of Eq. (51) with $m = 1$, the θ-component of Eq. (51) with $m = 2$, and Eq. (52) with $m = 2$, and can be summarized as follows:

$$\frac{\mathrm{d}}{\mathrm{d}\hat{r}}\left(\hat{r}\hat{\rho}_{H0}\hat{v}_{rH1}\right) = 0, \tag{53}$$

$$\frac{1}{2}\frac{\mathrm{d}\hat{p}_{H0}}{\mathrm{d}\hat{r}} - \frac{\hat{\rho}_{H0}\hat{v}^2_{\theta H0}}{\hat{r}} = 0, \tag{54}$$

$$\hat{r}\hat{\rho}_{H0}\hat{v}_{rH1}\frac{\mathrm{d}}{\mathrm{d}\hat{r}}\left(\hat{r}\hat{v}_{\theta H0}\right) = \frac{\mathrm{d}}{\mathrm{d}\hat{r}}\left[\hat{r}^2\hat{\mu}\frac{\hat{T}^{1/2}_{H0}}{2}\left(\frac{\mathrm{d}\hat{v}_{\theta H0}}{\mathrm{d}\hat{r}} - \frac{\hat{v}_{\theta H0}}{\hat{r}}\right)\right], \tag{55}$$

$$\begin{aligned}\hat{r}\hat{\rho}_{H0}\hat{v}_{rH1}\frac{\mathrm{d}}{\mathrm{d}\hat{r}}\left(\hat{v}^2_{\theta H0} + \frac{5}{2}\hat{T}_{H0}\right) =& \frac{\mathrm{d}}{\mathrm{d}\hat{r}}\left[\hat{r}\hat{\mu}\hat{T}^{1/2}_{H0}\hat{v}_{\theta H0}\left(\frac{\mathrm{d}\hat{v}_{\theta H0}}{\mathrm{d}\hat{r}} - \frac{\hat{v}_{\theta H0}}{\hat{r}}\right)\right.\\ &\left. + \hat{r}\hat{\lambda}\hat{T}^{1/2}_{H0}\frac{\mathrm{d}\hat{T}_{H0}}{\mathrm{d}\hat{r}} - k_T\frac{\hat{r}\hat{\rho}_{H0}\hat{v}_{rH1}\hat{T}_{H0}}{\chi^{A}_{H0}}\right],\end{aligned} \tag{56}$$

where

$$\begin{aligned}\hat{r}\hat{\rho}_{H0}\hat{v}_{rH1} =& -\hat{r}\frac{\hat{T}^{1/2}_{H0}}{\chi^{B}_{H0}}\left(\hat{D}_T\frac{\mathrm{d}\ln\hat{T}_{H0}}{\mathrm{d}\hat{r}} + \hat{D}_{AB}\frac{\mathrm{d}\chi^{A}_{H0}}{\mathrm{d}\hat{r}}\right)\\ &- 2(\hat{m}^B - \hat{m}^A)\hat{D}_{AB}\frac{\chi^{A}_{H0}}{\hat{T}^{1/2}_{H0}}\hat{v}^2_{\theta H0},\end{aligned} \tag{57}$$

$$\hat{\rho}_{H0} = \hat{m}^A\hat{n}^{A}_{H0} + \hat{m}^B\hat{n}^{B}_{H0}, \quad \hat{p}_{H0} = \hat{n}_{H0}\hat{T}_{H0}, \tag{58a}$$

$$\chi^{\alpha}_{H0} = \frac{\hat{n}^{\alpha}_{H0}}{\hat{n}_{H0}}, \quad \hat{n}_{H0} = \hat{n}^{A}_{H0} + \hat{n}^{B}_{H0}. \tag{58b}$$

The $\hat{\mu}$, $\hat{\lambda}$, k_T, $\hat{D}_T$, and $\hat{D}_{AB}$ in Eqs. (55)-(57), which are functions of $\hat{T}_{H0}$ and χ^{A}_{H0} (or χ^{B}_{H0}) and depend on the model of molecular interaction, correspond to the viscosity, thermal conductivity, thermal-diffusion ratio, thermal diffusion coefficient, and mutual diffusion coefficient, respectively. The definition of these transport coefficients is given in Appendix B. With Eqs. (58a) and (58b), Eqs. (53)–(57) form a closed set of equations for $\hat{n}^{A}_{H0}$, $\hat{n}^{B}_{H0}$, $\hat{v}_{rH1}$, $\hat{v}_{\theta H0}$, and $\hat{T}_{H0}$. Equations (53)-(56) are, respectively, the conservation equations for the total mass, the $\hat{r}$-component of the total momentum, its θ-component, and the total energy. Equation (57) expresses the diffusion in the radial direction.

In the derivation of the Hilbert solution, we have used the fact that the radial component of the flow velocity of the noncondensable gas is identically zero, which is a consequence of the boundary condition (27) on the cylinders. Except this, however, the boundary condition has not been taken into account so far. We now consider the boundary condition. Let us assume that the macroscopic variables $\hat{n}^{\alpha}_{H0}$, $\hat{v}_{\theta H0}$, and $\hat{T}_{H0}$ in f^{α}_{H0} take the following values on the surfaces of the cylinders; at $\hat{r} = 1$,

$$\hat{n}^{A}_{H0} = 1, \qquad \hat{v}_{\theta H0} = \frac{V_I}{V_{th}}, \qquad \hat{T}_{H0} = 1, \tag{59}$$

and at $\hat{r} = L_{II}/L_I$,

$$\hat{n}^A_{H0} = \frac{n_{II}}{n_I}, \qquad \hat{v}_{\theta H0} = \frac{V_{II}}{V_{th}}, \qquad \hat{T}_{H0} = \frac{T_{II}}{T_I}. \tag{60}$$

Then, because of the relation (30), it is seen that f^α_{H0} satisfies the boundary condition (27) at the leading order (the zeroth order in ϵ). The restrictions (59) and (60) give the consistent boundary conditions on the cylinders for the fluid-dynamic equations (53)-(58). Note that the boundary conditions (59) and (60) contain only the dimensionless parameters n_{II}/n_I, T_{II}/T_I, V_I/V_{th}, and V_{II}/V_{th} and do not depend on the reference quantity n_I or T_I.

The fluid-dynamic system, Eqs. (53)-(58) and Eqs. (59) and (60), gives the solution $\hat{n}^A_{H0}$, $\hat{n}^B_{H0}$, $\hat{v}_{rH1}$, $\hat{v}_{\theta H0}$, and $\hat{T}_{H0}$, with which the leading-order term f^α_{H0} is determined [Eq. (49)]. In this way, we obtain the leading-order solution of the boundary-value problem, Eqs. (17) and (27), by the Hilbert expansion.

3.2. Continuum limit and the ghost effect

Here, we give a brief remark on the behavior of the mixture in the continuum limit where Kn or ϵ vanishes. In this limit, the solution is given by Eq. (49), and the macroscopic variables reduce to their respective leading order terms, i.e., $(\hat{n}^A, \hat{n}^B, \hat{T}, \hat{v}_\theta, \hat{v}_r) \to (\hat{n}^A_{H0}, \hat{n}^B_{H0}, \hat{T}_{H0}, \hat{v}_{\theta H0}, 0)$ [cf. Eq. (48)]. That is, in this limit, evaporation and condensation of the vapor stop, and the radial component of the flow velocity $\hat{v}_r$ vanishes. Therefore, one might expect that the flow field in this limit is given by the flow field in the same limit of the ordinary cylindrical Couette flow of a binary mixture of noncondensable gases (or between impermeable cylinders). This is not true. The leading-order terms $\hat{n}^A_{H0}$, $\hat{n}^B_{H0}$, $\hat{T}_{H0}$, and $\hat{v}_{\theta H0}$ are determined together with the first-order term $\hat{v}_{rH1}$ of the radial component of the flow velocity. This means that, in spite of the fact that there is no evaporation or condensation, the flow field in the continuum limit is affected by the infinitesimal radial flow (or infinitesimal evaporation and condensation) [note that $\hat{v}_r = \hat{v}_{rH1}\epsilon + \cdots \to 0$, but $\hat{v}_{rH1}$ is of $O(1)$]. This is an example of the *ghost effect* that was pointed out in Ref. [11] and investigated extensively in subsequent works (see, Refs. [12–18] and the references in Refs. [15, 18]; for the case of a gas mixture, we refer to Refs. [19, 29–31]). In particular, the situation in the present problem is essentially the same as that of the plane Couette flow of the mixture of a vapor and a noncondensable gas [19]. Some numerical examples of the continuum limit obtained from the fluid-dynamic system, Eqs. (53)-(58) and Eqs. (59) and (60), will be given in Sec. 4.

In the case of the ordinary cylindrical Couette flow of a binary mixture of noncondensable gases, i.e., in the case where the A-component is also a noncondensable gas, the fluid-dynamic system can be derived readily by a slight modification of the analysis in the present section. The resulting fluid-dynamic equations are Eqs. (53)–(58) with $\hat{v}_{rH1} = 0$, and the boundary conditions are Eqs. (59) and (60) with the conditions for $\hat{n}^A_{H0}$ discarded. In this system, n_I, which appears in the nondimensionalization (16), should be regarded as an appropriate reference molecular number density, and n_{II} disappears. In addition, we have to specify a parameter associated with the amount of the A-component, say n^A_{av}/n_I with n^A_{av} being the average molecular number density of the A-component. Some numerical solution of this system (ordinary Couette flow, for short) will also be shown in the next section.

4. RESULTS AND DISCUSSIONS

In this section, we show some numerical results based on the fluid-dynamic system derived in Sec. 3 and discuss the behavior of the vapor and noncondensable gas in the continuum limit. We assume that both components consist of hard-sphere molecules. Therefore, since the fluid-dynamic boundary conditions do not depend on n_I or T_I, the problem is characterized by the dimensionless parameters n_{II}/n_I, T_{II}/T_I, V_I/V_{th}, V_{II}/V_{th}, n^B_{av}/n_I, L_{II}/L_I, m^B/m^A, and d^B/d^A. We let $T_{II}/T_I = 1$, $V_{II}/V_{th} = 0$, and $L_{II}/L_I = 2$ throughout this section. The relations between the terms $\hat{n}^\alpha_{H0}$, $\hat{v}_{\theta H0}$, $\hat{T}_{H0}$, etc. occurring in the fluid-dynamic system and the physical quantities

in the continuum limit are as follows:

$$\hat{n}^{\alpha}_{H0} = \frac{n^{\alpha}}{n_I}, \qquad \hat{\rho}_{H0} = \frac{\rho}{m^A n_I}, \qquad \hat{T}_{H0} = \frac{T}{T_I},$$
$$\hat{v}_{\theta H0} = \frac{v_\theta}{V_{th}}, \qquad \hat{v}_{rH1} = \lim_{\epsilon\to 0} \frac{v_r}{V_{th}} \frac{1}{\epsilon} = \lim_{\mathrm{Kn}\to 0} \frac{v_r}{V_{th}} \frac{2}{\sqrt{\pi}\mathrm{Kn}}, \tag{61}$$
$$\frac{2}{(L_{II}/L_I)^2 - 1} \int_1^{L_{II}/L_I} \hat{r}\hat{n}^B_{H0} \mathrm{d}\hat{r} = \frac{n^B_{av}}{n_I}.$$

4.1. Ghost effect

In Figs. 1 and 2, we show the profiles of the macroscopic quantities $\hat{n}^A_{H0}$, $\hat{n}^B_{H0}$, $\hat{v}_{\theta H0}$, $\hat{v}_{rH1}$, $\hat{\rho}_{H0}$, and $\hat{T}_{H0}$ for various values of n^B_{av}/n_I in the case $V_I/V_{th} = 0.5$, $m^B/m^A = 0.2$, and $d^B/d^A = 1$: Fig. 1 is for $n_{II}/n_I = 2$, and Fig. 2 for $n_{II}/n_I = 0.5$. In Fig. 1, infinitesimal evaporation takes place on the outer cylinder and infinitesimal condensation on the inner, so that there is an infinitesimal inward flow ($\hat{v}_{rII1} < 0$). In Fig. 2, the situation is opposite ($\hat{v}_{rII1} > 0$). The magnitude of the infinitesimal radial flow ($|\hat{v}_{rH1}\epsilon|$) increases as the amount of the noncondensable gas decreases, i.e., as n^B_{av}/n_I decreases. Correspondingly, the profile of the tangential velocity component ($\hat{v}_{\theta H0}$) is pushed inward (Fig. 1) or outward (Fig. 2) with the decrease of n^B_{av}/n_I. In Figs. 1 and 2, the results for the ordinary cylindrical Couette flow (i.e., the case where the A-component is also noncondensable) are also shown by dashed lines for the corresponding parameters, $V_I/V_{th} = 0.5$, $m^B/m^A = 0.2$, and $d^B/d^A = 1$. Here, the reference molecular number density n_I has been determined in such a way that the total number of the A-component, $n_I \int_1^2 \hat{r}\hat{n}^A_{H0} \mathrm{d}\hat{r}$, takes the same value as the corresponding case where the A-component is the vapor (see the last paragraph of Sec. 3.2). The $\hat{v}_{\theta H0}$ for the ordinary cylindrical Couette flow is practically independent of n^B_{av}/n_I, i.e., the concentration of the components.

We should now recall that there is no evaporation or condensation (i.e., the radial flow is infinitesimal) in the case of the mixture of a vapor and a noncondensable gas. However, the behavior is quite different from that of the ordinary cylindrical Couette flow. For example, the tangential velocity profile deviates significantly, and the deviation increases as n^B_{av}/n_I decreases. This deviation is due to the ghost effect caused by the infinitesimal evaporation and condensation.

We have also performed a Monte Carlo simulation for the original Boltzmann system, Eqs. (17) and (27), using the direct simulation Monte Carlo (DSMC) method [32, 33]. We have assumed the complete condensation condition for the vapor and the diffuse reflection condition for the noncondensable gas, i.e., Eq. (27) with Eqs. (32)–(35) and changed the Knudsen number Kn from 0.05 to 0.005. The results for the tangential and radial components of the flow velocity are shown in Figs. 3 and 4. Figure 3 corresponds to the case of Fig. 1 with $n^B_{av}/n_I = 0.2$, and Fig. 4 to the case of Fig. 2 with $n^B_{av}/n_I = 0.2$. As Kn is reduced, the magnitude of the radial component v_r decreases, showing the tendency that it vanishes in the limit $\mathrm{Kn} \to 0$. This is consistent with the fact that $\hat{v}_{rH0} = 0$ in the asymptotic analysis. On the other hand, the tangential component v_θ approaches the solid line that indicates the solution of the fluid-dynamic system. By the way, the dashed line indicates the solution of the fluid-dynamic system for the ordinary cylindrical Couette flow.

4.2. Bifurcation

Let us denote by M_r the mass flow of the vapor in the radial direction per unit time and per unit length of the axial coordinate z, which is infinitesimal in the continuum limit. Then, it is related to $\hat{\rho}_{H0}\hat{v}_{rH1}$ and $\hat{m}^A\hat{n}^A_{H0}\hat{v}^A_{rH1}$ as

$$\hat{r}\hat{\rho}_{H0}\hat{v}_{rH1} = \hat{r}\hat{m}^A\hat{n}^A_{H0}\hat{v}^A_{rH1} = \lim_{\mathrm{Kn}\to 0} \widetilde{M}, \qquad \widetilde{M} = \frac{M_r}{2\pi L_I m^A n_I V_{th}} \frac{2}{\sqrt{\pi}\mathrm{Kn}}, \tag{62}$$

where $\widetilde{M}$ is introduced for the later convenience. Figure 5 shows $\hat{r}\hat{\rho}_{H0}\hat{v}_{rH1}$ versus V_I/V_{th} for various values of n^B_{av}/n_I in the case $n_{II}/n_I = 1.5$, $m^B/m^A = 1$, and $d^B/d^A = 1$. When n^B_{av}/n_I is decreased

from 1 to 0.1, the curve becomes steep near $V_I/V_{th} = 1$, and the gradient of the curve there becomes negative with the further decrease of n_{av}^B/n_I. For example, for $n_{av}^B/n_I = 0.05$, there are three values of $\hat{r}\hat{\rho}_{H0}\hat{v}_{rH1}$ at the same V_I/V_{th} in a certain interval. In other words, the solution is not unique, and the bifurcation of the solution takes place. As n_{av}^B/n_I is decreased further, the curve tends to approach the dot-dashed curve that indicates the pure-vapor case [12]. In this special case of $m^B/m^A = d^B/d^A = 1$, all the curves pass the point $(V_I/V_{th}, \hat{r}\hat{\rho}_{H0}\hat{v}_{rH1}) = (1.0053, 0)$. The profiles of the tangential component $\hat{v}_{\theta H0}$ of the three solutions at $V_I/V_{th} = 1.0053$ for $n_{av}^B/n_I = 0.08$, 0.05, and 0.02 are shown in Fig. 6. The solution with $\hat{r}\hat{\rho}_{H0}\hat{v}_{rH1} = 0$ is common to all n_{av}^B/n_I and corresponds to the ordinary cylindrical Couette flow.

We have also performed a Monte Carlo simulation (DSMC) of the original Boltzmann system. Figure 7 shows the results for the case corresponding to Fig. 5. More specifically, $\widetilde{M}$ in Eq. (62) versus V_I/V_{th} is shown at Kn = 0.005 for $n_{av}^B/n_I = 0.5$, 0.05, and 0.02 in the case $n_{II}/n_I = 1.5$, $m^B/m^A = 1$, and $d^B/d^A = 1$. The corresponding curve in the continuum limit based on the fluid-dynamic system is also shown for comparison. The DSMC result demonstrates the nonuniqueness of the solution. However, we were not able to obtain the solution that roughly corresponds to the part of the curve with the negative gradient in Fig. 5. The solution on this part might be unstable. The profiles of the tangential velocity v_θ of the DSMC result corresponding to the points $(V_I/V_{th}, \widetilde{M}) = (1.0053, -3.36)$ and $(1.0053, 4.46)$ for $n_{av}^B/n_I = 0.05$ are shown in Fig. 8 together with the corresponding result in the continuum limit, i.e., $(V_I/V_{th}, \hat{r}\hat{\rho}_{H0}\hat{v}_{rH1}) = (1.0053, -4.643)$, $(1.0053, 0)$, and $(1.0053, 12.17)$.

In Figs. 7 and 8, the DSMC results at Kn = 0.005 still deviate significantly from the corresponding continuum limit. The discrepancy should reduce if we are able to carry out the DSMC computation for smaller Knudsen numbers. Although such a computation is seemingly easy in spatially one-dimensional problems such as the present one, in reality it is not an easy task because of the structure of the flow. When the Knudsen number is small, the Kn^0-order tangential velocity $\hat{v}_{\theta H0}$ is determined together with the Kn-order radial velocity $\hat{v}_{rH1}\epsilon$. Therefore, in the DSMC computation, we need to obtain the small radial velocity precisely in order to describe the tangential velocity correctly. As is well known, however, one of the drawbacks of the DSMC method is the difficulty in obtaining small quantities because they are buried in the statistical fluctuations inherent to the method. Since the radial velocity in the present problem decreases in proportion to the Knudsen number, the computation becomes increasingly difficult with the decrease of the Knudsen number.

Acknowledgments

The authors thank Prof. Shigeru Takata for his valuable discussions. This work is supported by the Grants-in-Aid for Scientific Research (Nos. 17360041 and 16001161) from JSPS and by the Center of Excellence for Research and Education on Complex Functional Mechanical Systems.

APPENDIX A: MACROSCOPIC QUANTITIES OF THE HILBERT EXPANSION

The explicit expressions of the macroscopic quantities of the Hilbert expansion by f_{Hm}^α are summarized. The coefficients of each gas h_{Hm}^α are

$$\hat{n}_{H0}^\alpha = \int f_{H0}^\alpha \mathrm{d}\boldsymbol{\zeta}, \tag{A1}$$

$$\hat{v}_{rH0}^\alpha = \frac{1}{\hat{n}_{H0}^\alpha} \int \zeta_r f_{H0}^\alpha \mathrm{d}\boldsymbol{\zeta}, \tag{A2}$$

$$\hat{v}_{\theta H0}^\alpha = \frac{1}{\hat{n}_{H0}^\alpha} \int \zeta_\theta f_{H0}^\alpha \mathrm{d}\boldsymbol{\zeta}, \tag{A3}$$

$$\begin{aligned} \hat{p}_{H0}^\alpha &= \hat{n}_{H0}^\alpha \hat{T}_{H0}^\alpha \\ &= \frac{2}{3} \int [(\zeta_r - \hat{v}_{rH0}^\alpha)^2 + (\zeta_\theta - \hat{v}_{\theta H0}^\alpha)^2 + \zeta_z^2] \hat{m}^\alpha f_{H0}^\alpha \mathrm{d}\boldsymbol{\zeta}, \end{aligned} \tag{A4}$$

and

$$\hat{n}^{\alpha}_{H1} = \int f^{\alpha}_{H1} \mathrm{d}\boldsymbol{\zeta}, \tag{A5}$$

$$\hat{v}^{\alpha}_{rH1} = \frac{1}{\hat{n}^{\alpha}_{H0}} \int \zeta_r f^{\alpha}_{H1} \mathrm{d}\boldsymbol{\zeta} - \frac{\hat{n}^{\alpha}_{H1}}{\hat{n}^{\alpha}_{H0}} \hat{v}^{\alpha}_{rH0}, \tag{A6}$$

$$\hat{v}^{\alpha}_{\theta H1} = \frac{1}{\hat{n}^{\alpha}_{H0}} \int \zeta_\theta f^{\alpha}_{H1} \mathrm{d}\boldsymbol{\zeta} - \frac{\hat{n}^{\alpha}_{H1}}{\hat{n}^{\alpha}_{H0}} \hat{v}^{\alpha}_{\theta H0}, \tag{A7}$$

$$\begin{aligned} \hat{p}^{\alpha}_{H1} &= \hat{n}^{\alpha}_{H0} \hat{T}^{\alpha}_{H1} + \hat{n}^{\alpha}_{H1} \hat{T}^{\alpha}_{H0} \\ &= \frac{2}{3} \int [(\zeta_r - \hat{v}^{\alpha}_{rH0})^2 + (\zeta_\theta - \hat{v}^{\alpha}_{\theta H0})^2 + \zeta_z^2] \hat{m}^{\alpha} f^{\alpha}_{H1} \mathrm{d}\boldsymbol{\zeta}. \end{aligned} \tag{A8}$$

The coefficients of the total mixture h_{Hm} are expressed in terms of those of each gas:

$$\hat{n}_{H0} = \hat{n}^{A}_{H0} + \hat{n}^{B}_{H0}, \tag{A9}$$

$$\hat{\rho}_{H0} = \hat{m}^{A} \hat{n}^{A}_{H0} + \hat{m}^{B} \hat{n}^{B}_{H0}, \tag{A10}$$

$$\hat{v}_{rH0} = \frac{1}{\hat{\rho}_{H0}} (\hat{m}^{A} \hat{n}^{A}_{H0} \hat{v}^{A}_{rH0} + \hat{m}^{B} \hat{n}^{B}_{H0} \hat{v}^{B}_{rH0}), \tag{A11}$$

$$\hat{v}_{\theta H0} = \frac{1}{\hat{\rho}_{H0}} (\hat{m}^{A} \hat{n}^{A}_{H0} \hat{v}^{A}_{\theta H0} + \hat{m}^{B} \hat{n}^{B}_{H0} \hat{v}^{B}_{\theta H0}), \tag{A12}$$

$$\hat{p}_{H0} = \hat{n}_{H0} \hat{T}_{H0} = \sum_{\alpha=A,B} \left[\hat{p}^{\alpha}_{H0} + \frac{2}{3} \hat{m}^{\alpha} \hat{n}^{\alpha}_{H0} (V^{\alpha}_{rH0})^2 + \frac{2}{3} \hat{m}^{\alpha} \hat{n}^{\alpha}_{H0} (V^{\alpha}_{\theta H0})^2 \right], \tag{A13}$$

and

$$\hat{n}_{H1} = \hat{n}^{A}_{H1} + \hat{n}^{B}_{H1}, \tag{A14}$$

$$\hat{\rho}_{H1} = \hat{m}^{A} \hat{n}^{A}_{H1} + \hat{m}^{B} \hat{n}^{B}_{H1}, \tag{A15}$$

$$\hat{v}_{rH1} = \frac{1}{\hat{\rho}_{H0}} \left[\sum_{\alpha=A,B} (\hat{m}^{\alpha} \hat{n}^{\alpha}_{H0} \hat{v}^{\alpha}_{rH1} + \hat{m}^{\alpha} \hat{n}^{\alpha}_{H1} \hat{v}^{\alpha}_{rH0}) - \hat{\rho}_{H1} \hat{v}_{rH0} \right], \tag{A16}$$

$$\hat{v}_{\theta H1} = \frac{1}{\hat{\rho}_{H0}} \left[\sum_{\alpha=A,B} (\hat{m}^{\alpha} \hat{n}^{\alpha}_{H0} \hat{v}^{\alpha}_{\theta H1} + \hat{m}^{\alpha} \hat{n}^{\alpha}_{H1} \hat{v}^{\alpha}_{\theta H0}) - \hat{\rho}_{H1} \hat{v}_{\theta H0} \right], \tag{A17}$$

$$\begin{aligned} \hat{p}_{H1} &= \hat{n}_{H0} \hat{T}_{H1} + \hat{n}_{H1} \hat{T}_{H0} \\ &= \sum_{\alpha=A,B} \left\{ \hat{p}^{\alpha}_{H1} + \frac{2}{3} \hat{m}^{\alpha} \hat{n}^{\alpha}_{H1} \left[(V^{\alpha}_{rH0})^2 + (V^{\alpha}_{\theta H0})^2 \right] + \frac{4}{3} \hat{m}^{\alpha} \hat{n}^{\alpha}_{H0} \left(V^{\alpha}_{rH0} V^{\alpha}_{rH1} + V^{\alpha}_{\theta H0} V^{\alpha}_{\theta H1} \right) \right\}, \end{aligned} \tag{A18}$$

where

$$V^{\alpha}_{rHm} = \hat{v}^{\alpha}_{rHm} - \hat{v}_{rHm}, \quad V^{\alpha}_{\theta Hm} = \hat{v}^{\alpha}_{\theta Hm} - \hat{v}_{\theta Hm}. \tag{A19}$$

APPENDIX B: HILBERT SOLUTION f^{α}_{H1}

In this appendix the index γ is used to represent the labels A and B of the gas species, in addition to α and β. The first-order Hilbert solution f^{α}_{H1} is given in the following form:

$$\begin{aligned} f^{\alpha}_{H1} = f^{\alpha}_{H0} \Bigg[& \frac{\hat{p}^{\alpha}_{H1}}{\hat{p}^{\alpha}_{H0}} + 2\hat{m}^{\alpha} \frac{\hat{v}_{rH1} \tilde{\zeta}_r + \hat{v}_{\theta H1} \tilde{\zeta}_\theta}{\hat{T}^{1/2}_{H0}} + \frac{\hat{T}_{H1}}{\hat{T}_{H0}} \left(\hat{m}^{\alpha} \tilde{\zeta}^2 - \frac{5}{2} \right) \\ & - \tilde{\zeta}_r A^{\alpha}(\tilde{\zeta}) \frac{1}{\hat{p}_{H0}} \frac{\mathrm{d}\hat{T}_{H0}}{\mathrm{d}\hat{r}} - \tilde{\zeta}_r \tilde{\zeta}_\theta B^{\alpha}(\tilde{\zeta}) \frac{\hat{T}^{1/2}_{H0}}{\hat{p}_{H0}} \left(\frac{\mathrm{d}\hat{v}_{\theta H0}}{\mathrm{d}\hat{r}} - \frac{\hat{v}_{\theta H0}}{\hat{r}} \right) \\ & - \tilde{\zeta}_r \sum_{\beta=A,B} D^{(\beta)\alpha}(\tilde{\zeta}) \frac{1}{\hat{n}_{H0} \hat{p}_{H0}} \left(\frac{\mathrm{d}\hat{p}^{\beta}_{H0}}{\mathrm{d}\hat{r}} - \frac{2\hat{m}^{\beta} \hat{n}^{\beta}_{H0} \hat{v}^2_{\theta H0}}{\hat{r}} \right) \Bigg], \end{aligned} \tag{B1}$$

where

$$\tilde{\zeta}_r = \frac{\zeta_r}{\hat{T}_{H0}^{1/2}}, \quad \tilde{\zeta}_\theta = \frac{\zeta_\theta - \hat{v}_{\theta H0}}{\hat{T}_{H0}^{1/2}}, \quad \tilde{\zeta}_z = \frac{\zeta_r}{\hat{T}_{H0}^{1/2}}, \quad \tilde{\zeta}^2 = \tilde{\zeta}_r^2 + \tilde{\zeta}_\theta^2 + \tilde{\zeta}_z^2. \tag{B2}$$

The functions $A^\alpha(\zeta)$, $B^\alpha(\zeta)$, and $D^{(\beta)\alpha}$ are the solutions of the following integral equations:

$$\left.\begin{aligned} &\sum_{\beta=A,B} K^{\beta\alpha}\chi_{H0}^{\beta}\tilde{L}_T^{\beta\alpha}(\zeta_r A^\beta, \zeta_r A^\alpha) = -\zeta_r\left(\hat{m}^\alpha\zeta^2 - \frac{5}{2}\right), \\ &\text{subsidiary condition:} \quad \sum_{\alpha=A,B} \hat{m}^\alpha\chi_{H0}^{\alpha} I_4^\alpha(A^\alpha) = 0, \end{aligned}\right\} \tag{B3}$$

$$\sum_{\beta=A,B} K^{\beta\alpha}\chi_{H0}^{\beta}\tilde{L}_T^{\beta\alpha}(\zeta_r\zeta_\theta B^\beta, \zeta_r\zeta_\theta B^\alpha) = -2\hat{m}^\alpha\zeta_r\zeta_\theta, \tag{B4}$$

$$\left.\begin{aligned} &\sum_{\beta=A,B} K^{\beta\alpha}\chi_{H0}^{\alpha}\chi_{H0}^{\beta}\tilde{L}_T^{\beta\alpha}(\zeta_r D^{(\gamma)\beta}, \zeta_r D^{(\gamma)\alpha}) = -\zeta_r\left(\delta_{\alpha\gamma} - \frac{\hat{m}^\alpha n_{H0}^\alpha}{\hat{\rho}_{H0}}\right), \\ &\text{subsidiary condition:} \quad \sum_{\alpha=A,B} \hat{m}^\alpha\chi_{H0}^{\alpha} I_4^\alpha(D^{(\beta)\alpha}) = 0, \end{aligned}\right\} \tag{B5}$$

where $\zeta = (\zeta_r^2 + \zeta_\theta^2 + \zeta_z^2)^{1/2}$. The operators $\tilde{L}_T(f,g)$ and $I_n(F)$ is defined as follows:

$$\tilde{L}_T^{\beta\alpha}(f,g) = \int [f(\zeta_*') + g(\zeta') - f(\zeta_*) - g(\zeta)] E^\beta(\zeta_*)\hat{B}_T^{\beta\alpha}\mathrm{d}\Omega(\mathbf{e})\mathrm{d}\boldsymbol{\zeta}_*, \tag{B6}$$

$$\hat{B}_T^{\beta\alpha} = \hat{B}_T^{\beta\alpha}(|\mathbf{e}\cdot\hat{\boldsymbol{V}}|/\hat{V}, \hat{V}) = \hat{B}^{\beta\alpha}\left(|\mathbf{e}\cdot\hat{\boldsymbol{V}}|/\hat{V}, \hat{V}\hat{T}_{H0}^{1/2}\right)/\hat{T}_{H0}^{1/2}, \tag{B7}$$

$$I_n^\alpha(F) = \frac{8\pi}{15}\left(\frac{\hat{m}^\alpha}{\pi}\right)^{3/2}\int_0^\infty \zeta^n F(\zeta)\exp(-\hat{m}^\alpha\zeta^2)\mathrm{d}\zeta, \tag{B8}$$

where

$$E^\beta(\zeta_*) = \left(\frac{\hat{m}^\beta}{\pi}\right)^{3/2}\exp\left(-\hat{m}^\beta\zeta_*^2\right), \tag{B9}$$

$$\zeta_* = (\zeta_{*r}^2 + \zeta_{*\theta}^2 + \zeta_{*z}^2)^{1/2}. \tag{B10}$$

The transport coefficients $\hat{\mu}$, $\hat{\lambda}$, k_T, $\hat{D}_T$, and $\hat{D}_{AB}$ in Eqs. (55)-(57) are defined by means of the functions A^α, B^α, and $D^{(\gamma)\alpha}$ as follows:

$$\left.\begin{aligned} &\hat{D}_{AB} = \chi_{H0}^A\chi_{H0}^B\left(\hat{\Delta}_{AA} + \hat{\Delta}_{BB} - \hat{\Delta}_{AB} - \hat{\Delta}_{BA}\right), \\ &\hat{D}_T = \chi_{H0}^A\chi_{H0}^B\left(\hat{D}_{TA} - \hat{D}_{TB}\right), \\ &\hat{\mu} = \textstyle\sum_{\alpha=A,B}\hat{m}^\alpha\chi_{H0}^\alpha\hat{\mu}^\alpha, \\ &k_T = \frac{\hat{D}_T}{\hat{D}_{AB}}, \quad \hat{\lambda} = \hat{\lambda}' - k_T\frac{\hat{D}_T}{\chi_{H0}^A\chi_{H0}^B}, \end{aligned}\right\} \tag{B11}$$

where

$$\left.\begin{aligned} &\hat{\Delta}_{\alpha\beta} = \frac{5}{2}I_4^\alpha\left(D^{(\beta)\alpha}\right), \\ &\hat{D}_{T\alpha} = \frac{5}{2}I_4^\alpha\left(A^\alpha\right), \\ &\hat{\mu}^\alpha = \hat{m}^\alpha I_6^\alpha\left(B^\alpha\right), \\ &\hat{\lambda}'^\alpha = \frac{5}{2}I_4^\alpha\left(\left[\hat{m}^\alpha\zeta^2 - \frac{5}{2}\right]A^\alpha\right). \end{aligned}\right\} \tag{B12}$$

From the subsidiary conditions and appropriate integration of the integral equations in Eqs (B3), (B5), the following relations are derived, with the help of which the form of Eqs. (55)-(57) is obtained:

$$\hat{\Delta}_{\alpha\beta} = \hat{\Delta}_{\beta\alpha}, \tag{B13}$$

$$\sum_{\beta=A,B} \hat{m}^{\beta} \chi^{\beta}_{H0} \hat{\Delta}_{\alpha\beta} = 0, \tag{B14}$$

$$\sum_{\beta=A,B} \hat{m}^{\beta} \chi^{\beta}_{H0} \hat{D}_{T\beta} = 0. \tag{B15}$$

A numerical database for the coefficients $\hat{\mu}$, $\hat{\lambda}$, k_T, $\hat{D}_T$, and $\hat{D}_{AB}$ for hard-sphere molecules has been constructed in Ref. [34], and it has been used in obtaining the numerical solution presented in Sec. 4.

---

[1] C. Cercignani and F. Sernagiotto, Phys. Fluids **10**, 1200 (1967).
[2] K. Nanbu, Phys. Fluids **27**, 2632 (1984).
[3] F. Sharipov and G. Kremer, Eur. J. Mech. B/Fluids **15**, 493 (1996).
[4] K. Aoki, H. Yoshida, T. Nakanishi, and A. L. Garcia, Phys. Rev. E **68**, 016302 (2003).
[5] Y. Sone, H. Sugimoto, and K. Aoki, Phys. Fluids **11**, 476 (1999).
[6] Y. Sone, T. Ohwada, and Y. Makihara, in *Rarefied Gas Dynamics*, edited by R. Brun, R. Campargue, R. Gatignol, and J.-C. Lengrand (Cépaduès-Éditions, Toulouse, 1999), Vol. 1, p. 511.
[7] Y. Sone and T. Doi, Phys. Fluids **12**, 2639 (2000).
[8] Y. Sone, M. Handa, and H. Sugimoto, Transp. Theory Stat. Phys. **31**, 299 (2002).
[9] L. Arkeryd and A. Nouri, J. Stat. Phys. **118**, 849 (2005).
[10] K. Aoki and Y. Sone, in *Advances in Kinetic Theory and Continuum Mechanics*, edited by R. Gatignol and Soubbaramayer (Springer-Verlag, Berlin, 1991), p. 43.
[11] Y. Sone, K. Aoki, S. Takata, H. Sugimoto, and A. V. Bobylev, Phys. Fluids **8**, 628 (1996); Erratum: *ibid* **8**, 841 (1996).
[12] Y. Sone, S. Takata, and H. Sugimoto, Phys. Fluids **8**, 3403 (1996); Erratum: *ibid* **10**, 1239 (1998).
[13] Y. Sone, in *Rarefied Gas Dynamics*, edited by Ching Shen (Peking University Press, Beijing, 1997), p. 3.
[14] Y. Sone, Annu. Rev. Fluid Mech. **32**, 779 (2000).
[15] Y. Sone, *Kinetic Theory and Fluid Dynamics* (Birkhäuser, Boston, 2002).
[16] Y. Sone, M. Handa, and T. Doi, Phys. Fluids **15**, 2903 (2003).
[17] Y. Sone and T. Doi, Phys. Fluids **16**, 952 (2004).
[18] Y. Sone, *Molecular Gas Dynamics: Theory, Techniques, and Applications* (Birkhäuser, Boston, 2006).
[19] S. Takata and K. Aoki, Phys. Fluids **11**, 2743 (1999).
[20] C. Cercignani, *Rarefied Gas Dynamics* (Cambridge University Press, 2000).
[21] C. Cercignani and M. Lampis, Transp. Theory Stat. Phys **1**, 101 (1971).
[22] Y. Sone, in *Rarefied Gas Dynamics*, edited by L. Trilling and H. Y. Wachman (Academic Press, New York, 1969), p. 243.
[23] Y. Sone, in *Rarefied Gas Dynamics*, edited by D. Dini (Editrice Tecnico Scientifica, Pisa, Italy, 1971), Vol. II, p. 737.
[24] Y. Sone, in *Advances in Kinetic Theory and Continuum Mechanics*, edited by R. Gatignol and Soubbaramayer (Springer, Berlin, 1991), p. 19.
[25] S. Chapman and T. G. Cowling, *The Mathematical Theory of Non-Uniform Gases*, 3rd Ed. (Cambridge University Press, Cambridge, 1995).
[26] K. Aoki, S. Takata, and S. Taguchi, Eur. J. Mech. B/Fluids **22**, 51 (2003).
[27] K. Aoki, S. Takata, and S. Kosuge, Phys. Fluids **10**, 1519 (1998).
[28] S. Taguchi, K. Aoki, and S. Takata, Phys. Fluids **16**, 4105 (2004).
[29] S. Takata, K. Aoki, and T. Muraki, in *Rarefied Gas Dynamics*, edited by R. Brun, R. Campargue, R. Gatignol, and J.-C. Lengrand (Cépaduès-Éditions, Toulouse, 1999), Vol. 1, p.479.
[30] S. Takata and K. Aoki, Transp. Theory Stat. Phys. **30**, 205 (2001); **31**, 289(E) (2002).
[31] S. Takata, Phys. Fluids **16**, 2182 (2004).
[32] G. A. Bird, *Molecular Gas Dynamics* (Oxford University Press, Oxford, 1976).
[33] G. A. Bird, *Molecular Gas Dynamics and the Direct Simulation of Gas Flows* (Oxford University Press, Oxford, 1994).
[34] S. Takata, S. Yasuda, K. Aoki, and T. Shibata, in *Rarefied Gas Dynamics*, edited by A. D. Ketsdever and E. P. Muntz (Melville, New York, 2003), p.106.

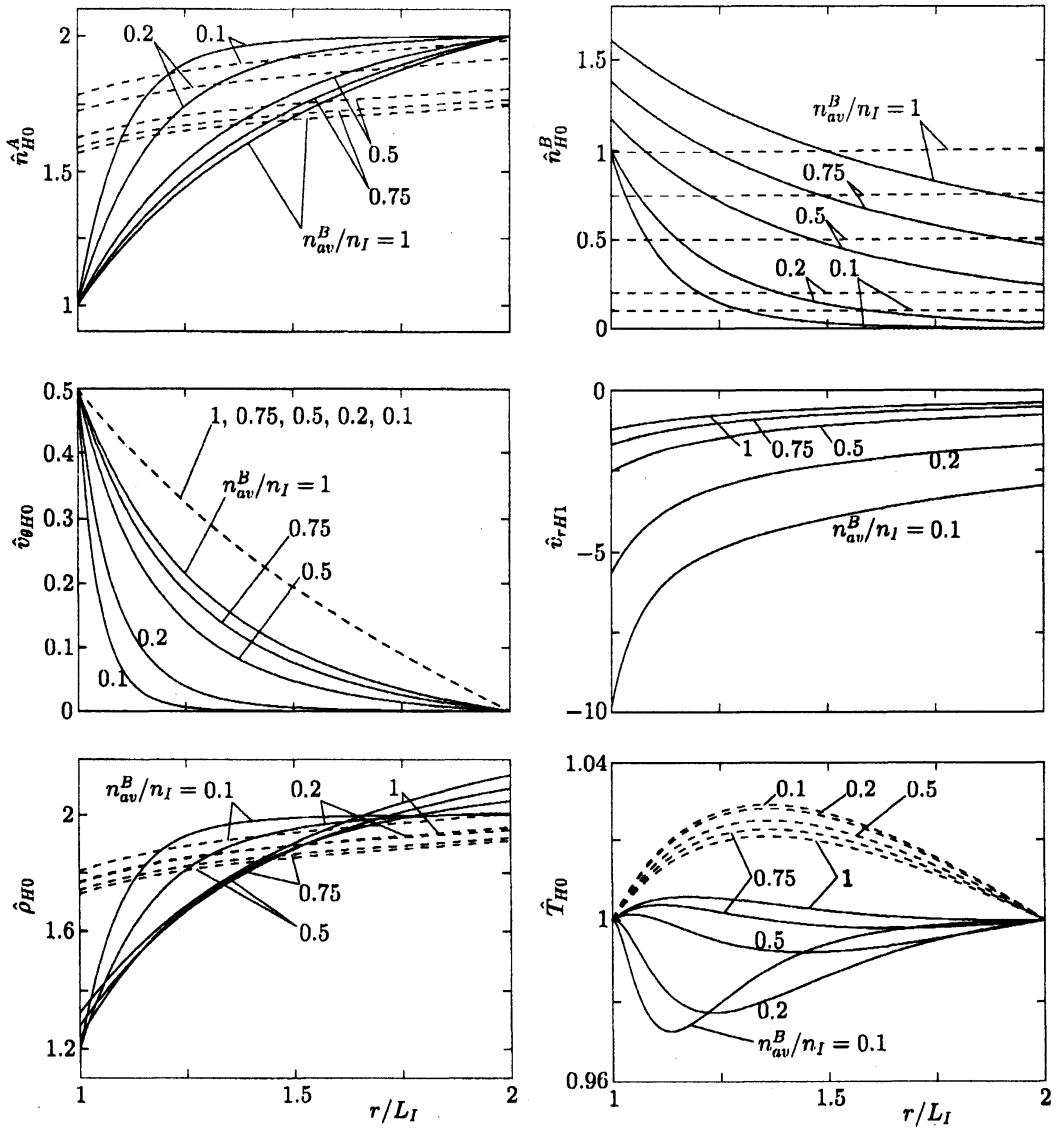

FIG. 1: Profiles of the macroscopic quantities in the continuum limit for various n^B_{av}/n_I (hard-sphere molecules) in the case of $n_{II}/n_I = 2$, $V_I/V_{th} = 0.5$, $m^B/m^A = 0.2$, and $d^B/d^A = 1$ ($L_{II}/L_I = 2$, $T_{II}/T_I = 1$, and $V_{II} = 0$). The dashed line indicates the corresponding results for ordinary cylindrical Couette flow (see the main text for the meaning of n_I in this case).

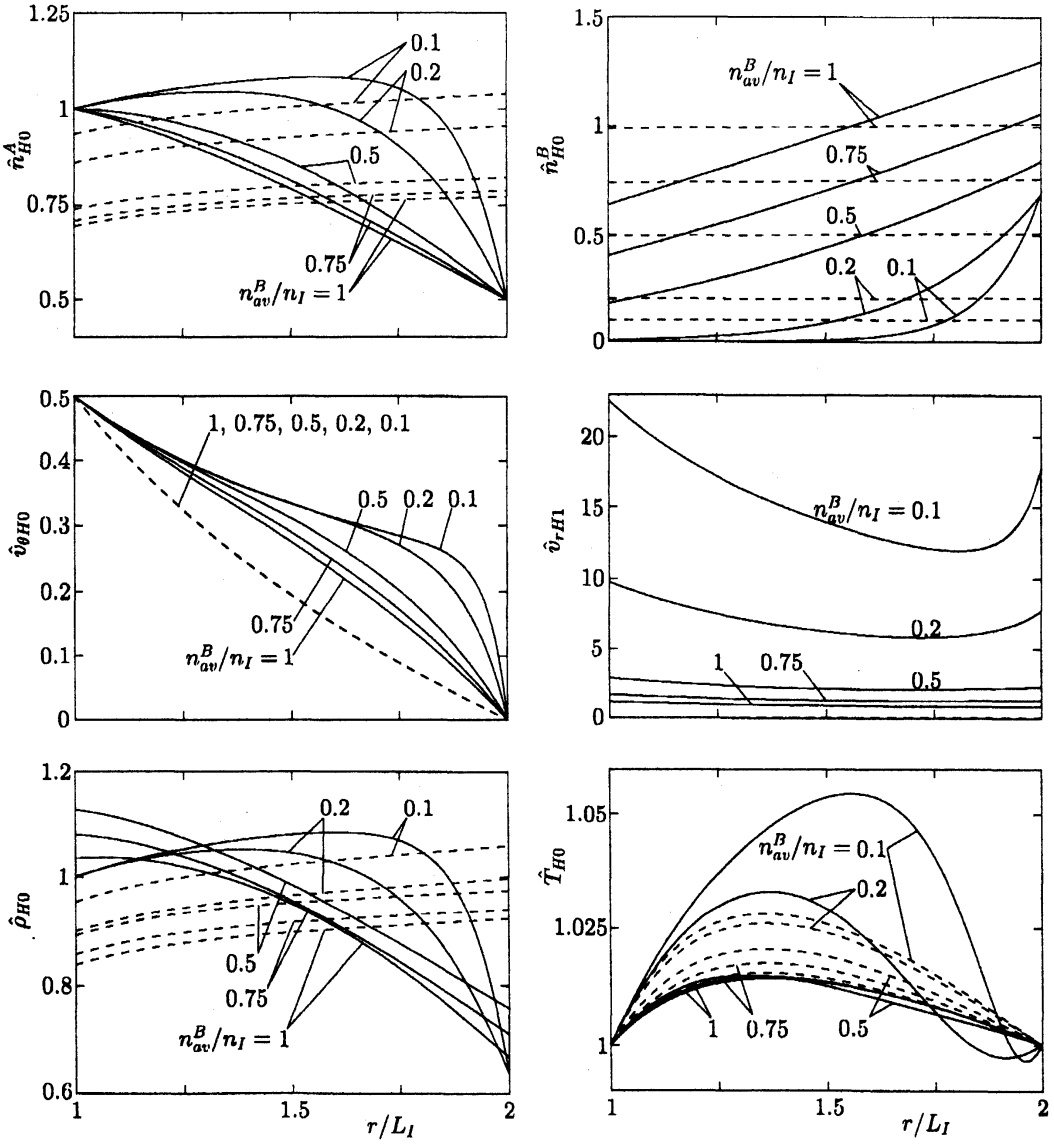

FIG. 2: Profiles of the macroscopic quantities in the continuum limit for various n^B_{av}/n_I (hard-sphere molecules) in the case of $n_{II}/n_I = 0.5$, $V_I/V_{th} = 0.5$, $m^B/m^A = 0.2$, and $d^B/d^A = 1$ ($L_{II}/L_I = 2$, $T_{II}/T_I = 1$, and $V_{II} = 0$). See the caption of Fig. 1.

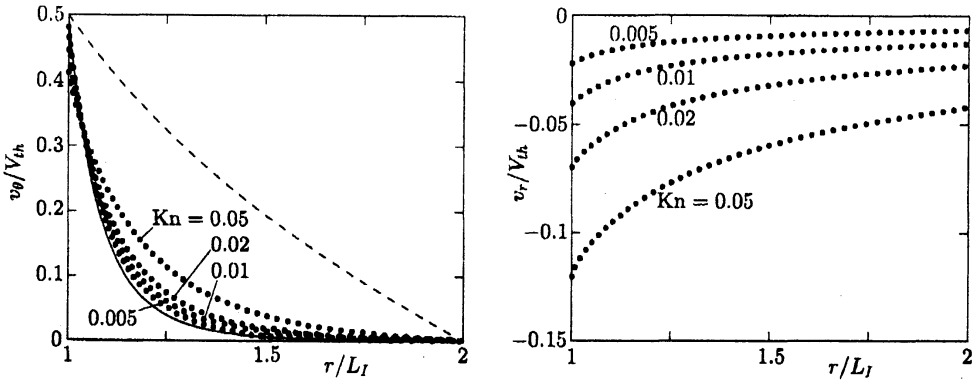

FIG. 3: Profiles of the flow velocity for small Kn (DSMC result for hard-sphere molecules) in the case of $n^B_{av}/n_I = 0.2$, $n_{II}/n_I = 2$, $V_I/V_{th} = 0.5$, $m^B/m^A = 0.2$, and $d^B/d^A = 1$ ($L_{II}/L_I = 2$, $T_{II}/T_I = 1$, and $V_{II} = 0$). The solid line indicates the profile of the continuum limit, and the dashed line that of the same limit for the ordinary cylindrical Couette flow.

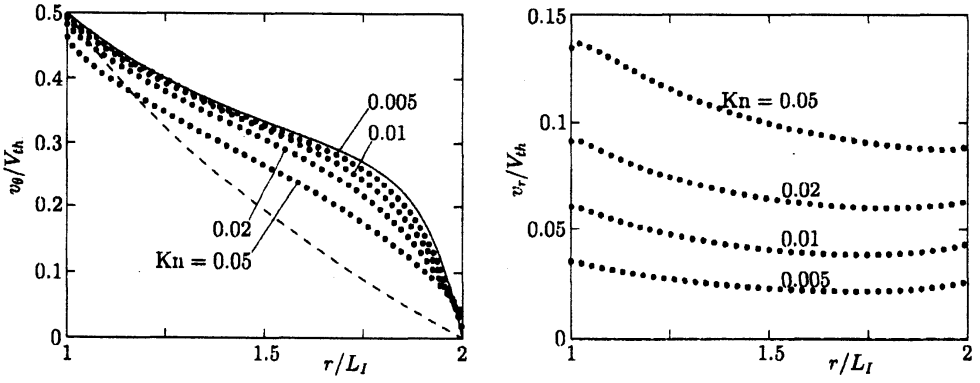

FIG. 4: Profiles of the flow velocity for small Kn (DSMC result for hard-sphere molecules) in the case of $n^B_{av}/n_I = 0.2$, $n_{II}/n_I = 0.5$, $V_I/V_{th} = 0.5$, $m^B/m^A = 0.2$, and $d^B/d^A = 1$ ($L_{II}/L_I = 2$, $T_{II}/T_I = 1$, and $V_{II} = 0$). See the caption of Fig. 4.

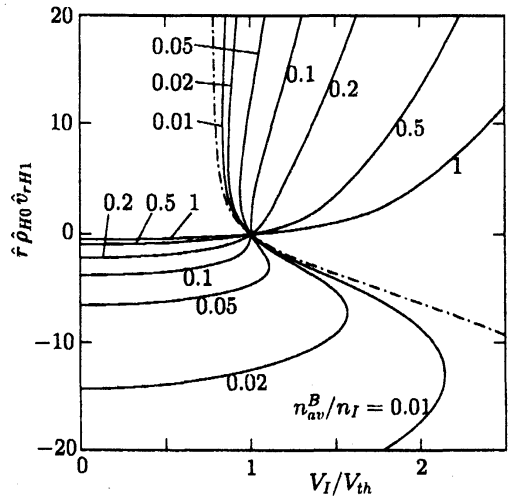

FIG. 5: The $\hat{r}\hat{\rho}_{H0}\hat{v}_{rH1}$ versus V_I/V_{th} in the continuum limit for various n^B_{av}/n_I (hard-sphere molecules) in the case of $n_{II}/n_I = 1.5$, $m^B/m^A = 1$, and $d^B/d^A = 1$ ($L_{II}/L_I = 2$, $T_{II}/T_I = 1$, and $V_{II} = 0$). The dot-dashed line indicates the pure vapor case [12].

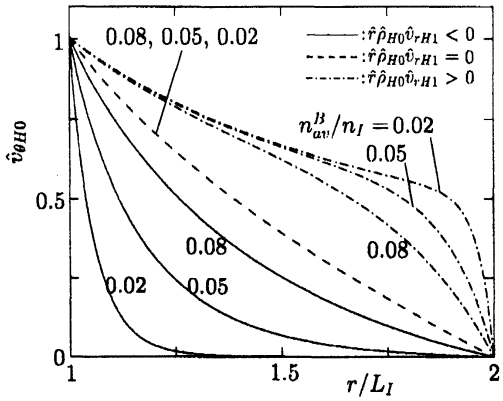

FIG. 6: Profiles of $\hat{v}_{\theta H0}$ of the three different solutions in the continuum limit at $V_I/V_{th} = 1.0053$ (hard-sphere molecules) for $n^B_{av}/n_I = 0.08$, 0.05, and 0.02 in the case of $n_{II}/n_I = 1.5$, $m^B/m^A = 1$, and $d^B/d^A = 1$ ($L_{II}/L_I = 2$, $T_{II}/T_I = 1$, and $V_{II} = 0$).

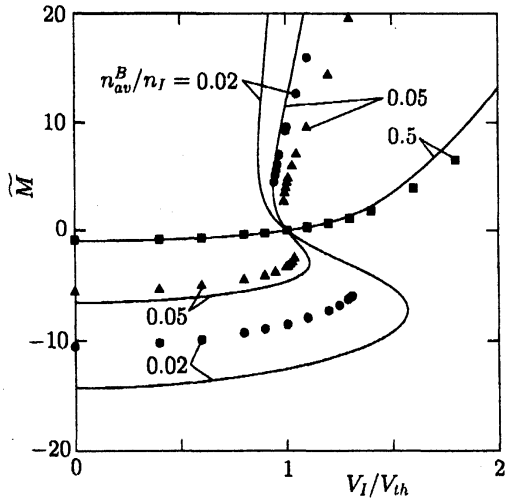

FIG. 7: Magnified mass flow rate $\widetilde{M}$ versus V_I/V_{th} at Kn = 0.005 (DSMC result for hard-sphere molecules) for $n^B_{av}/n_I = 0.5$, 0.05, and 0.02 in the case of $n_{II}/n_I = 1.5$, $m^B/m^A = 1$, and $d^B/d^A = 1$ ($L_{II}/L_I = 2$, $T_{II}/T_I = 1$, and $V_{II} = 0$). The solid line indicates the results in the continuum limit.

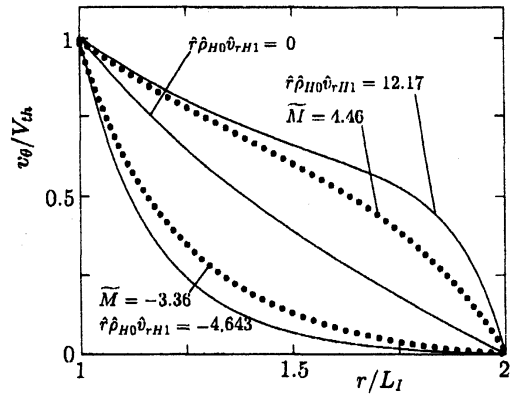

FIG. 8: Profiles of the tangential velocity v_θ at Kn = 0.005 (DSMC result for hard-sphere molecules) corresponding to $(V_I/V_{th}, \widetilde{M}) = (1.0053, -3.36)$ and (1.0053, 4.46) in the case of $n^B_{av}/n_I = 0.05$, $n_{II}/n_I = 1.5$, $m^B/m^A = 1$, and $d^B/d^A = 1$ ($L_{II}/L_I = 2$, $T_{II}/T_I = 1$, and $V_{II} = 0$). The corresponding results in the continuum limit, i.e., the profiles at $(V_I/V_{th}, \hat{r}\hat{\rho}_{H0}\hat{v}_{rH1}) = (1.0053, -4.643)$, (1.0053, 0), and (1.0053, 12.17), are also shown by the solid line.